4

Optochemical Sensor Systems for *In-Vivo* Continuous Monitoring of Blood Gases in Adipose Tissue and in Vital Organs

Merima Čajlaković[1], Alessandro Bizzarri[1], Gijs H. Goossens[2], Igor Knez[3], Michael Suppan[1], Ismar Ovčina[3] and Volker Ribitsch[1]
[1]*Joanneum Research Forschungsgesellschaft mbH, MATERIALS - Institute for Surface Technologies and Photonic, Sensorsystems, Graz,*
[2]*Department of Human Biology, NUTRIM School for Nutrition, Toxicology and Metabolism, Maastricht University Medical Centre, Maastricht,*
[3]*Department of Cardiac Surgery, University Clinic of Surgery, Medical University Graz, Graz,*
[2]*The Netherlands*
[1,3]*Austria*

1. Introduction

Sensors capable of determining both oxygen and carbon dioxide partial pressure, as well as pH in blood, are of particular interest with respect to the medical care of critically ill patients. Those parameters are informative indicators of the conditions of a living system and can be valuable in determining the physiologic status of critically ill patients. Tissue oxygenation represents the balance between local oxygen delivery and consumption. Under resting conditions the level varies between and within organs; it is lower in more metabolically active tissues, such as brain (Hou et al., 2003), liver (Vollmar et al., 1992), renal cortex and medulla Whitehouse et al., 2006) and higher in tissues with low metabolic rates, such as the bladder (Rosser et al., 1995, 1996). Changes in blood carbon dioxide levels are associated with myocardial acidosis and alkalosis, ventricular fibrillation and reduced myocardial contractility in addition to providing an indication of cardiac resuscitability (Maldonado et al., 1993; Tang et al., 1996). The respiratory gases themselves reflect cardiopulmonary homeostasis. This is the ability of the cardiopulmonary system to maintain a constant relationship between respiration in the cells of the body, the supply of oxygen from the lungs to the blood and the elimination of carbon dioxide by the lungs. In this way, partial pressures of O_2 and CO_2 are kept at their normal physiological values. Thus, the body constantly consumes oxygen and produces carbon dioxide, and there is a normal balance between the absolute contents and the partial pressures of these gases in the blood (Hahn, 1998). Although this balance can be upset by many clinical or physiological factors, the cardiopulmonary function has a remarkable ability to compensate for these changes, especially to maintain the gases at their normal values. The magnitude of the arterial blood pCO_2 is the key clinical measure of the effectiveness of the lungs to expel CO_2. Therefore, it is clinically important to measure the inspired and expired partial pressures of both oxygen

and carbon dioxide in the critically ill adult and infant patient. It is possible either to take a blood sample and analyse this in the laboratory, what is routinely done in hospitals, or to perform the measurement *in vivo*. Although a number of methods are used in the clinical setting to measure blood gases, including blood gas analysis and electrodes (Astrup, 1986; Harsten, 1988; Suzuki, 1999), some practical issues restrict their use, e.g. the distance of the analyzer from the bedside, the need for special training of clinicians and staff for proper blood sample collection and handling, potential contamination of blood samples by the biological medias and the sensitivity of the method. Thus, there is huge need and interest to develop more sensitive and practical methodologies such as optical techniques, especially in the field of *in vivo* intravascular blood-gas analysis (Suzuki, 2001; Tsukada, 2003; Tusa, 2001; Wolfbeis, 1991). *In vivo* gas sensors should respond rapidly, preferably with a response time of the order of seconds, if the measurements are to have any significant physiological meaning. So far, the only commercially available sensors for the monitoring of adipose tissue oxygen partial pressure pO_2 are needle-type sensors. Those suffer of the typical drawbacks of a point measurement, which is strongly dependent on the position of the sensor tip inside the adipose tissue and show high fragility due to the small dimension of the sensor heads.

Combination of the optical sensor with a microdialysis technique is a powerful tool for online monitoring of metabolism in tissues (Cooney, 1997, 2000; Ungerstedt, 1991). This is mainly due to the fact that the subcutaneous adipose tissue is easily accessible and the risk of infection is low. The microdialysis probe, which is a hollow fibre which functions as an artificial blood vessel, is inserted into the tissue and is perfused with a dialysis solvent. Exchange of substances between the microdialysis probe and the extracellular fluid (sample medium) occurs over a semi-permeable membrane. Low molecular weight substances in the interstitial fluid surrounding the microdialysis catheter are allowed to diffuse across the membrane and to equilibrate with the perfusion solution. The interstitial fluid leaves the probe via a side arm from which it is collected (Goossens et al., 2011). Optical sensing approach combined with microdialysis have been already used for monitoring of dissolved gases and pH in a flow loop (Cooney, 1997, 2000). Pasic et al. (Pasic et al., 2006) have described a microdialysis-based glucose-sensing system with an integrated fibre-optic hybrid sensor. An important advantage of this system is that for example adipose tissue pO_2 is measured over a much larger area compared to commercially available needle-type oxygen sensors.

In our first work we reported on optical capillary sensors for continuous measurement of oxygen and carbon dioxide in subcutaneous tissue using microdialysis for extraction of interstitial fluid in subcutaneous tissue (Bizzarri, 2006; Cajlakovic, 2006). The adopted sensing scheme for both sensors was phase fluorometry, which is based on the dynamic quenching due to oxygen of the photo-excited luminophore Platin(II) meso-tetra(pentafluorophenyl) porphyrin (Pt-TFPP). In the case of carbon dioxide sensor an ion-pairing approach combined with dual luminophore referencing as a detection technique was used for the preparation of carbon dioxide sensitive layers. The analysis of extracted sample by means of the external instrumentation is properly designed for rapid analysis of small volumes (less than microliters) and allowed a less invasive technique than the intravascular approach (Bizzarri, 2006; Cajlakovic, 2006). Recently, we have presented an improved optochemical measurement system for continuous monitoring of adipose tissue oxygen tension in biological fluid using a miniaturized flow-through cell instead of a

capillary-based sensor coupled to a microdialysis catheter (Bizzarri, 2007; Cajlakovic, 2009). The effectivness and accuracy of the sensors were investigated *in vitro* using physiological solution (ringer) and *in vivo* tests in order to examine the magnitude of changes in tissue gas tension in response to evolving shock and resuscitation: 1) on test animals, where hemorrhagic schock model has been adopted to simulate critically condition and 2) on healthy volunteers, where infusion of adrenaline caused the changes in tissue oxygenation. Adipose tissue oxygen tension may be involved in the development of insulin resistance (impaired action of the hormone insulin) in humans. Therefore the continuous monitoring of adipose tissue oxygen tension (pO_2) in individuals affected by obesity and/or type 2 diabetes mellitus is highly interesting. Recent cell culture and preclinical experiments suggest that obesity is accompanied by low levels of oxygen in adipose tissue (Ye et al., 2007). However, this concept was recently challenged by Goossens et al. (Goossens et al., 2011), demonstrating increased adipose tissue PO2 in obese insulin resistant compared to lean insulin sensitive men. The optochemical sensor technology combined with microdialysis is particularly suitable for the development of minimally invasive instrumentation for measurement of tissue pO_2 (Goossens et al., 2011). In the present chapter, we present an improved microdialysis-based oxygen-sensing instrumentation with integrated planar sensitive membrane inserted in a miniaturised flow-through-cell (volume app. 5µl) for the continuous monitoring of adipose tissue oxygen tension in humans. This instrumentation is suitable for measurement at a flow rate as low as 2 µl/min with a response time, including the flow time from the catheter to the sensitive membrane, of about 10 min. The sensor system has been validated in *in vivo* experiments, in which adipose tissue oxygen tension in humans has been monitored under resting conditions and after the local administration of a vasoconstrictor and vasodilator (Goossens et al., 2011). As expected, local administration of the vasoconstrictor in adipose tissue decreased both adipose tissue blood flow and adipose tissue pO_2. Subsequently, local infusion of the vasodilator increased both adipose tissue blood flow and pO_2 values (Goossens et al., 2011). Obtained results showed good agreement between the observed adipose tissue oxygen tension and the expected behavior due to the induced alteration of adipose tissue blood flow. Thus, this system is suitable for in vivo monitoring of pO_2 in adipose tissue.

The second part of this contribution includes the description of the optochemical measurement system for simultaneously monitoring of tissue O_2 and CO_2 partial pressure in brain, heart and liver by means of miniaturized implanted fiber optical sensor. pO_2 and pCO_2 measurements are based on the determination of the luminescence lifetime via phase modulation fluorometry. The instrumentation unit consists of two independent channels for measuring pO_2 and pCO_2. The O_2 sensor is based on the luminescent dye Pt-pentafluorophenyl-porphyrin, while for CO_2 sensor the Resonant Energy Transfer (RET) scheme is used to convert the intensity of the analyte dependent dye indicator into long luminescence lifetime information, which can be measured by phase modulation fluorometry (Lakowicz, 1983). Therewith it was for the first time possible to measure continuously and simultaneously O_2 and CO_2 content in brain, heart and liver during open-heart surgery. Fiber optical sensors have been tested in an experimental animal model during cardiac surgery using two different methods as extra corporal circulation: conventional cardiopulmonary bypass (CPB) and minimal extracorporeal circulation systems (mini-EEC). CPB is the most accepted surgical technique to treat cardiac pathologies. It is a safe and established technique with a low mortality rate (Pentila et al.,

2001). However, besides neurological events, which may at least be partially related to the use of CPB, and the inflammatory response, the ideal myocardial protection is still a matter of scientific and clinical debate (Chang, 2002; Immer, 2005; Levy, 2003). Mini-ECC system consists of a centrifugal pump, an oxygenator and a modified suction system. The main advantage of mini-ECC is the reduction of tubing length (reduction of the priming volume). It was designed to reduce blood tubing, the contact between blood and air and priming volume during cardiac surgery. The main issue of developing miniaturised extracorporeal circulation systems is the strong need for a CPB concept for cardiac surgery which will cause fewer traumas to blood components and reduce the extensive volume shifts and bubble formation during cardiopulmonary bypass (Kofidis et al., 2008). A closed circuit, where the patient himself/herself serves as a reservoir with a minimized priming volume, could be the ideal alternative to reduce the adverse effects of CPB (Kamiya et al., 2006). In a complex, technically demanding, prospective, randomized and blinded experimental setting, an extracorporeal circulation has been performed using mini-EEC versus standard CPB techniques with main emphasis on differences in organ specific oxygen and carbon dioxide partial pressures and metabolism. *In-vivo* experiments on animals with implanted optical O_2 and CO_2 sensors were performed in order to be able to establish if there is any difference in O_2/CO_2 metabolism when using two types of extracorporeal circulation, CPB and mECC, respectively.

2. The continuous monitoring of adipose tissue oxygen tension (pO_2) in humans

2.1 Design of an optical oxygen sensor

The luminophore Platin(II) meso-tetra(pentafluorophenyl) porphyrin (Pt-TFPP) was used because of its long lifetime (~ 50 ms), strong absorption in green region of the spectrum, which is compatible with green light-emitting diodes (LEDs), its highly emissive metal-to-ligand charge transfer state and its high photostability. The dye was entrapped in a hydrophobic polymer of polystyrene (4 w. % dye/g solid polystyrene in chloroform). Afterwards the sensor cocktail was spread onto a transparent substrate; either a polyethylene terephthalate foils PET (Mylar foil with thickness 100 μm) or PET foils (50 μm thickness) coated with Al_2O_3. Knife coating and screen printing techniques have been used for production. After coating, the oxygen sensitive membranes have been dried at 60 °C for eight hours. In the case of knife coating a successive mechanical reduction of the sensitive spot to a diameter of 2 mm has been applied. This procedure was not necessary in case of the screen printed sensitive membranes.

2.2 Measurement principle

The luminescence lifetime of a luminophore is an intrinsic property and is independent of for example detector sensitivity and fluctuations in light intensity therefore phase fluorometry was used as sensing scheme. In this case the luminophore is excited by sinusoidally modulated light at a given frequency ω and the emitted sinusoidal luminescence is also modulated at the same frequency. The lifetime of the luminophore causes a time lag between the absorbance and emission, expressed by the phase angle θ and a decreased intensity relative to the incident light, called demodulation. The relationship

between the lifetime τ and the phase shift ϕ for a single exponential decay is given by equation (1) and is illustrated in Fig. 1:

$$\tau = \frac{tan\phi}{2\pi f} \tag{1}$$

where f is the modulation frequency. An optimal frequency need to be selected because signal-to-noise (SNR) ratio decreases and phase sensitivity increases with increasing modulation frequency. The used luminophore was Pt-TFPP, whose luminescence is dynamic quenched (reduced) in the presence of oxygen and subsequently the lifetime as well. The optimal frequency for this dye was chosen 4.5 kHz. The instrumentation measures the phase shift of the luminescence with respect to the excitation signal. This is related to the luminescence lifetime of the dye, which in turn depends on the pO_2 of the tissue in contact with the surface of the sensor probe. The pO_2 can be calculated from the measured phase shift of the luminescence using the so called false-light model (Bizzarri et al., 2006) as described by equation (2):

$$\phi = \phi_0 \left[\frac{f_0}{1 + K \cdot pCO_2} + 1 - f_0 \right] \tag{2}$$

where ϕ is the phase shift measured at a given oxygen partial pressure pO_2, ϕ_0 is the phase shift in absence of O_2, K is the quenching parameter and f_0 is the false-light parameter (the fraction of the luminescence emitted by the sensor, which is quenched by oxygen).

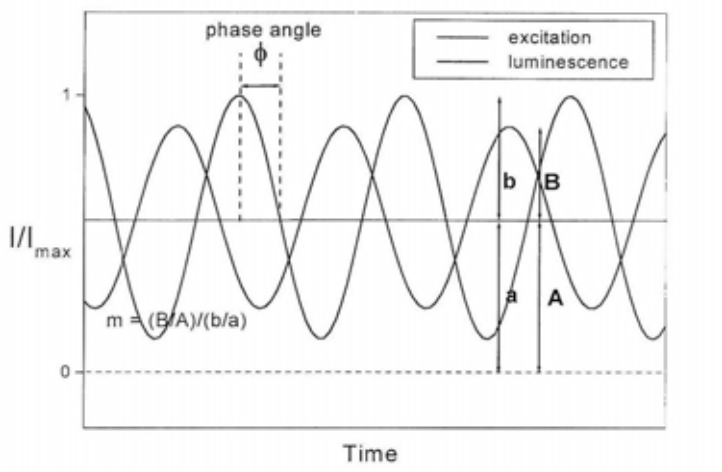

Fig. 1. Principle of phase fluorimetric technique. Luminescence emission is delayed in phase angle Φ and demodulated relative to the excitation (m).

2.3 Miniaturised flow-through cell and optoelectronic measurement unit

The fibre optic measurement system consists of an optoelectronic read-out module for measurements with optical fibres (core diameter 1000 µm) and of a miniaturised flow-

through cell (volume app. 5 µl), where a planar oxygen sensitive membrane (diameter of the sensitive spot 2 mm) is allocated. The measurement set-up is shown in Fig. 2. The flow through cell is equipped with inlet tubing of inner diameter of 0.15 mm and outer diameter of 0.30 mm (Rometch GmbH). The outlet tubing and the flow chamber have an inner diameter of 2.0 mm. The outer diameter of the outlet tubing is 3.0 mm as presented in Fig. 3. The inner diameter of the inlet was chosen to be 0.15 mm in order to match the inner diameter of the inlet of the microfluidic catheter. This geometry has been chosen to reduce the risk of overpressure during measurement, which would cause an overestimation of the dissolved pO_2. The length of the inlet is 20 mm whereas the outlet is 32 mm long. The tubings are made of stainless steel in order to prevent or to reduce the permeation of ambient oxygen to non-significant values.

Fig. 2. Measurement system for planar sensing membranes. The flow-through cell has a size of 20 x 13 x 4.8 mm (length x width x heigth). The measuring chamber of the flow-through-cell has a diameter of circa 1.8 mm and a height of about 2.8 mm, thus resulting in a volume of about 5 µl. The sensing membranes have a round sensitive spot of 1.8 mm in diameter.

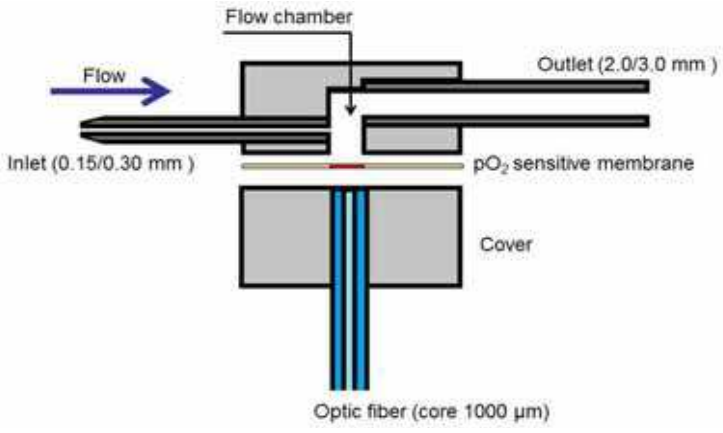

Fig. 3. Schematic draw of the flow through cell

The optic set-up is integrated in the processing electronic unit and is based on a collimating optics, which converts the light of the excitation source (a Nichia NSPE590S LED) into a parallel beam. This is then focused by a GRIN lens into an optic fibre, which guides the excitation light to the oxygen sensitive layer inside the flow-through cell. The luminescence collected by the same optic fibre is deflected by a dichroic filter at 45 ° (DC Red, Qioptiq Photonics GmbH & Co. KG) towards the detector a silicon photodiode (Hamamatsu S5106). A set of optical filters (SCHOTT BG39, thickness 2 mm, for the excitation source and SCHOTT RG630, thickness 2 mm, for the photodiode) is used to separate the luminescence signal from the excitation light and other optical background signals (e.g. luminescence emitted by materials close to the O_2 sensitive membrane). A reference light source (Nichia NSPE590S LED) is used to compensate the reading of the measuring unit for changes of the electronic parameters of the components with fluctuations of the operating conditions (e.g. forward current through the LED and temperature). The main advantage of using fiber optic technology is the possibility to separate the optoelectronic instrumentation from the flow-through cell, thus allowing an extreme miniaturization of the cell itself. The new flow-through-cell has size of only 20 x 13 x 4.8 mm, which makes it more flexible for use in *in vivo* experiments and use in hospitals. In order to prevent disconnection of the fluidic when the patient moves the flow-through cell was mounted on a belt for fixed positioning on the abdomen of the subject during *in vivo* experiment, as it is shown in Fig. 4.

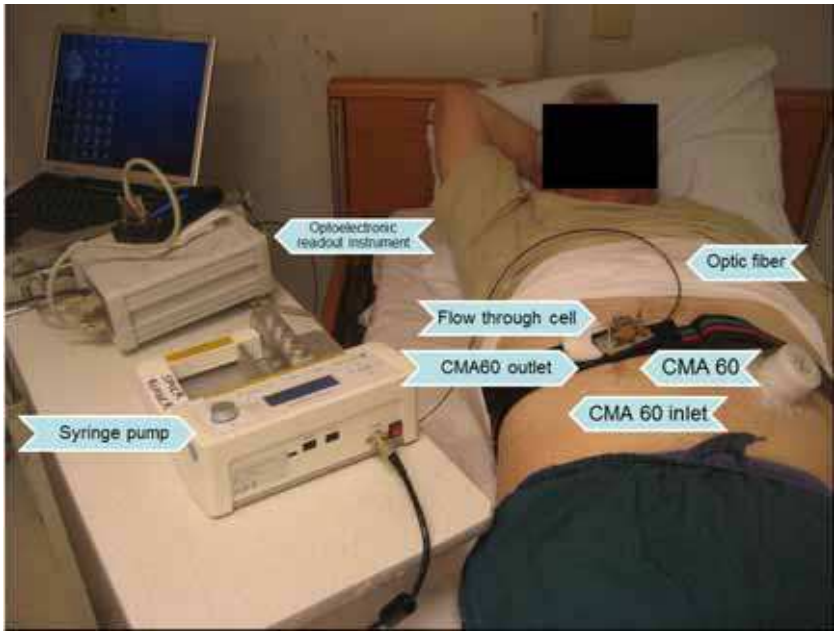

Fig. 4. Use of the optochemical oxygen sensor instrumentation during a typical in vivo experiment. The main components are the flow-through-cell, which is fixed near the umbilicus of the volunteer close to the position of insertion of the CMA 60 microdialysis catheter. The luminescence emitted by the oxygen sensitive membrane is collected by an optic fibre cable and guided to the optoelectronic read-out unit. The microdialysis probe is perfused using a microinfusion syringe pump. These experiments were carried out in the laboratory of Dr. G.H. Goossens (Maastricht University Medical Centre, The Netherlands).

For the extraction of interstitial fluid microdialysis catheter CMA60 was used. The outlet tubing of catheter was first cut as close as possible to the microdialysis membrane (at a distance of about 2 mm) and then connected with the flow through cell by means of steel tubing (diameters 0.15/0.30 mm). The length of the steel tubing was standardised at 90 mm in each experiment. In this way the ambient oxygen diffusion through the permeable tubing materials of the catheter can be neglected. This has been proven in oxygen recovery rate measurements, which have been carried out in laboratory. These measurements have been already exhaustively described in previously reported work (Cajlakovic et al., 2009). The standardization of the length of all the connection tubing allows that the flow time from the catheter to the sensitive membrane is in all experiments the same.

2.4 Applications and practical systems

2.4.1 Sensor performance and laboratory calibration protocol

The membranes have been produced by knife coating technique onto PET substrate and by means of screen printing onto PET substrate coated with Al_2O_3 as oxygen barrier.

All sensor membranes have been firstly laboratory characterized in Ringer solution (physiological solution used as perfusate in many clinical procedures) at temperature held constant at 37 °C. The temperature regulation was realised by using a water bath thermostat (Lauda RC 6 CP). The measurement medium has been equilibrated with a gas mixture of nitrogen and oxygen at defined concentrations (typically 0, 5, 10 and 21 % O_2) using a mass flow controller (Bronkhorst, The Netherlands). A paramagnetic gas purity analyser (Servomex, U.K.) was served as reference instrumentation. The solution was then pumped by means of a peristaltic pump into a miniaturised flow-through cell at the flow rate of 2.0 µl/min (Minipuls 3, Gilson, Germany). One example of a typical sensor response curve, phase angle as a function of different O_2 concentrations, is shown in Fig. 5.

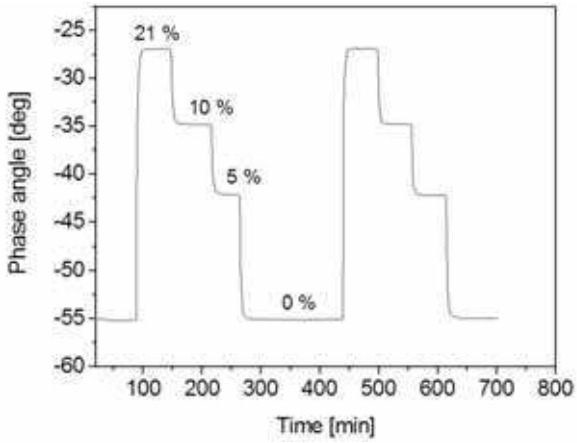

Fig. 5. Example of the experimental protocol used for the characterisation of the miniaturised planar O_2 sensitive membrane. The measurement is carried out in Ringer solution equilibrated at defined O_2 concentrations (0, 5, 10 and 21 % O_2) at the constant temperature of 37 °C.

Two cycles have been performed, whereas the first complete cycle of dissolved O_2 was used for sensor calibration purpose, and the following cycle is used to check the specifications of the oxygen measurement (Table 1).

	Specifications
Working range	0-300 mmHg
Resolution	1 mmHg
Accuracy	< 7% or ±1 mmHg

Table 1. Achieved specifications of the O_2 measurement with planar sensitive membranes compared to the optimum requirements defined in the project

Both types of membranes perform satisfactorily with the same measurement specifications.

2.4.2 Delay time

The time needed for the extracted interstitial fluid to reach the sensitive oxygen membrane in the flow-through cell is indicated as delay time. This delay time is defined as the time required for the sensor output to change from its previous state to a final settled value within a tolerance band of the new value. It is a common practice to measure the delay time as the time needed for the sensor to reach the 90 % of the final output. This is usually indicated as the t_{90} of the sensor. Fig. 6 shows the delay time t90 for an oxygen change from air saturated solution (circa 21 % O_2) to oxygen free solution (about 0 %).

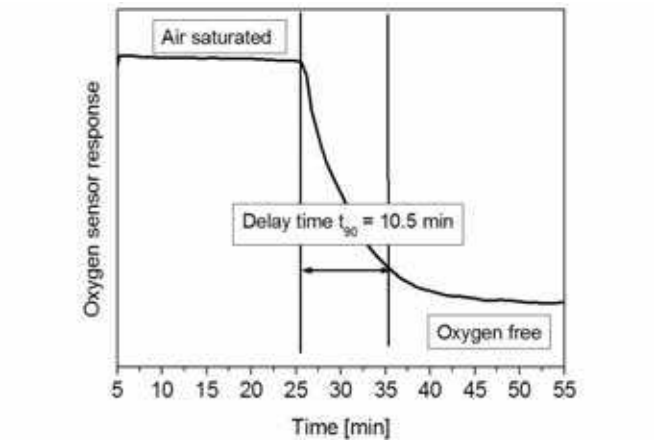

Fig. 6. Measured delay time between 21 and 0 % of O_2 in case of one oxygen sensitive membrane

To perform this measurement, two different glass vessels filled with Ringer solution has been equilibrated with air and nitrogen. The catheter CMA 60 connected by steel tubing to the flow through cell has been first immersed in the vessel containing air saturated Ringer solution and the peristaltic pump was started with flow rate of 2 µl/min. After a stable value of the oxygen sensor instrumentation has been achieved, the pump has been shortly stopped to change the catheter in the oxygen free Ringer solution and the flow started again. The time needed to achieve the 90% of the final value as been recorded. Six different

membranes of both types have been investigated and the averaged t_{90} could be estimated as 11.7 ± 4.6 min. Even if, the two different types of sensitive membranes (based on uncoated or Al_2O_3 coated PET substrate) perform satisfactorily with regard to the measurement specifications, it could be observed that, in single membranes based on the uncoated PET substrate, the response time increased above the specified time of 10 min, due to ambient oxygen diffusion through microscopic damages of the coated surface, caused by the mechanical reduction of the sensitive spot.

2.4.3 Clinical validation in humans

2.4.3.1 Validation protocol

To validate the sensor instrumentation for *in vivo* use in humans, a healthy, normal-weight male subject participated in an experiment carried out at Maastricht University Medical Centre in The Netherlands. The subject was asked to refrain from drinking alcohol and to perform no strenuous exercise for a period of 48 hours before the *in vivo* experiment. On arrival, a microdialysis catheter (CMA 60, CMA microdialysis AB, Stockholm, Sweden) was inserted in the abdominal subcutaneous adipose tissue 6 cm right from the umbilicus after the skin was anesthetized by a lidocaine/prilocaine cream (EMLA, AstraZeneca BV, Zoetermeer, The Netherlands). After insertion, the probe was perfused with Ringer solution (Baxter BV, Utrecht, The Netherlands), supplemented with 50 mM ethanol, at a flow rate of 2.0 µl/min (CMA400 micro infusion pump, CMA microdialysis AB, Stockholm, Sweden). Afterwards, the system was allowed to equilibrate. After pO_2 had reached stable values, the probe was consecutively perfused with a vasoconstrictor and vasodilator, each for 60 min. There was a wash-out period of 120 min (Ringer infusion) before the infusion of the vasodilator was started.

2.4.3.2 Results and discussion of *in vivo* measurement of adipose tissue oxygen tension in humans

A stable baseline pO_2 of 52.5 mmHg was reached after 2-3 hours (Fig. 7, time -30 to 0 min). As hypothesized, local administration of a vasoconstrictor in adipose tissue (t0-60 min) decreased both adipose tissue blood flow and adipose tissue pO_2 (37.3 mmHg, Figure 7). During the wash-out period (t60-180min) the probe was perfused with Ringer solution, and pO_2 values returned to near-baseline values again (53.5 mmHg). Subsequently, local infusion of a vasodilator increased both adipose tissue blood flow and pO_2 values to 74.8 mmHg (t180-240min). This experiment clearly showed that pO_2 values can be reliably measured *in vivo* in humans, and can be modified by changes in tissue blood flow. These results have been extensively described elsewhere (Goossens et al., 2011).

The rapid increase of the measured pO_2 at the beginning of each drug administration (spikes in Fig.7) is caused by ambient oxygen, which has been introduced in the fluidic during the change of the infusion solution.

After the *in vivo* experiments several oxygen sensitive membranes were recalibrated in the laboratory, and the deviations of the pO_2 values obtained by the second calibration were calculated and plotted against the actual pO_2 values (Fig. 8). Importantly, the change in the calibration of the sensitive membrane after the *in vivo* experiment causes very small discrepancy (<0.5 mmHg) from the actual pO_2 values. This result is excellent considering that the oxygen sensitive membranes have been recalibrated about one year after the first laboratory calibration and after in vivo experiments of a typical duration of 5 – 8 hours.

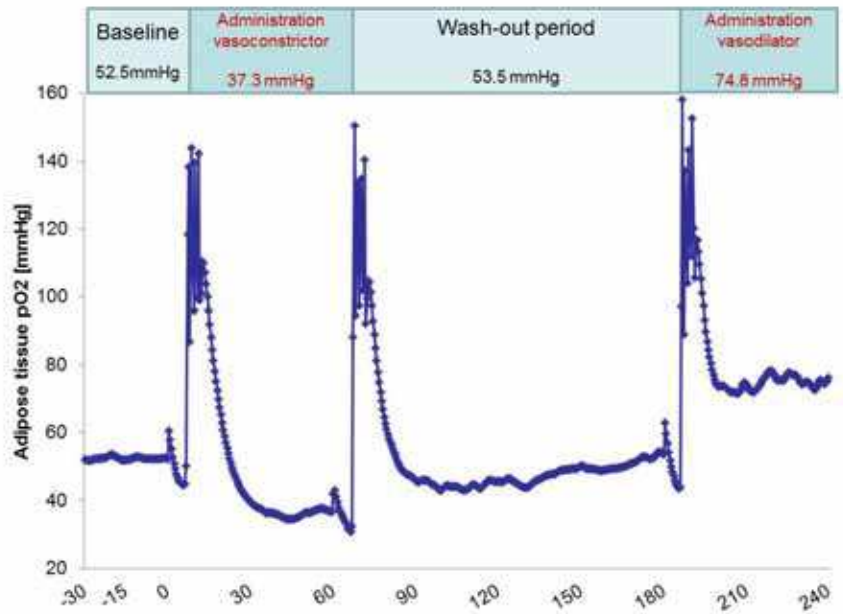

Fig. 7. Measured abdominal adipose tissue pO_2 with optochemical sensitive membrane under stable baseline conditions (local Ringer administration up to time 0), during local administration (2 µl/min) of a vasoconstrictor between 0 and 60 min, followed by wash-out period with Ringer infusion (from 60 to 180 min). At 180 min an infusion of a vasodilator was started up to 240 min. The experiment was carried out in the laboratory of Dr. G.H. Goossens (Maastricht University Medical Centre, The Netherlands) (Goossens et al., 2011).

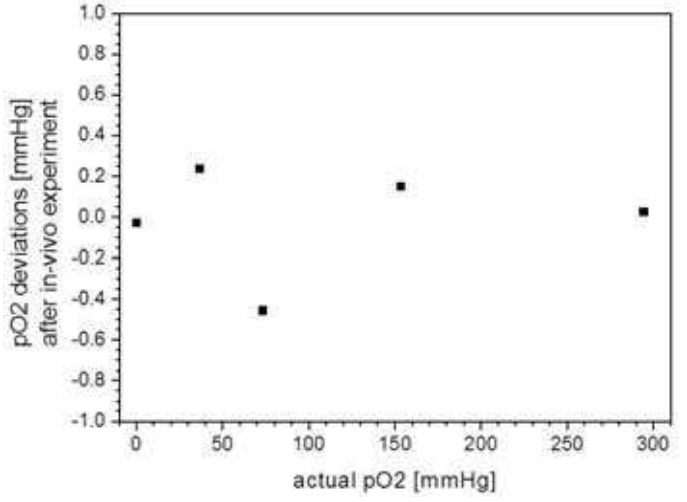

Fig. 8. Deviations of the pO_2 values measured for single oxygen sensitive membrane after in vivo experiments compared to the calibration values.

2.5 Conclusion

We have developed and validated a microdialysis-based oxygen-sensing instrumentation with integrated miniaturized sensitive membrane for the continuous monitoring of adipose tissue oxygen tension in humans. In comparison to previously reported instrumentation (Cajlakovic et al., 2009), this system can be used at a flow rate as low as 2 µl/min with a response time of about 10 min (including the flow time from the catheter to the sensitive membrane). The production technology of the oxygen sensitive membranes has been improved, allowing the pO_2 measurement in the range between 0 and 300 mmHg with accuracy better than ±1 mmHg and resolution better than 1 mmHg. The system has been validated *in vivo*, where adipose tissue oxygen tension has been monitored in humans under resting conditions and during local administration of vasoactive compounds. Local administration of the vasoconstrictor in adipose tissue decreased adipose tissue pO_2 and subsequently, local infusion of the vasodilator increased pO_2 in adipose tissue (Goossens et al., 2011). The agreement between the observed adipose tissue oxygen tension and the expected behaviour after modulation of adipose tissue blood flow allows concluding that the system is suitable for in vivo monitoring of pO_2 in humans. Several sensitive membranes were recalibrated after in vivo experiments in the laboratory and deviations smaller than ± 0.5 mmHg were observed. This indicates that the membranes have an excellent storage and operating stability, and that contact with biological fluid does not affect the read-out of the optochemical measurement instrumentation.

2.6 Acknowledgement

The in vivo experiments in humans were carried out at Maastricht University Medical Centre, Maastricht, The Netherlands, under supervision of Dr. G. H. Goossens.

3. Optochemical measurement system for simultaneously monitoring of O_2 and CO_2 partial pressure in vital organs by means of miniaturized implanted fibre optical sensor

The measurement system is composed of two channels allowing simultaneously measuring of O_2 and CO_2 partial pressures (pO_2 and pCO_2). The optoelectronic measurement unit for O_2 is same as described in chapter 2 (Paragraph 2.3). For this application optical fibres were coated with sensitive layers (O_2 and CO_2). In the case of using an optical fibre as support for the sensitive layer, pulses of light emitted by a green (in the case of O_2 sensor) or blue LED (in the case of CO_2 sensor) are carried via an optical fiber to excite the dye at the sensor tip. On interaction with measured parameter the luminescence is quenched and is transmitted back within the same fibre to the detection unit. The instrumentation measures the phase shift of the luminescence with respect to the excitation signal.

3.1 Optoelectronic measurement unit for CO_2

As in the case of the O_2 measurement channel a measurement system for CO_2 is based on a collimating optics to convert the light of excitation source (Nichia NSPB500) into a parallel beam, which can be focused by a GRIN lens into the optic fibre. The luminescence collected by the optic fibre is also transformed by the same GRIN lens into a parallel beam, which is deflected by a dichroic filter at 45 ° (Unaxis B51) with respect to the optical axis to the silicon photodiode as a photo-detector (Hamamatsu S5106). Dichroic filters transmit selected ranges of the visible spectrum and reflect the complementary ranges, thus they may be used

to separate the radiation emitted by the excitation source from the luminescence. Additional glass optical filters (SCHOTT BG12, thickness 2 mm for the excitation source and SCHOTT KV550, thickness 3 mm as emission filter) are used to separate the luminescence from stray light and optical background due to the excitation source. For the compensation of the reading of the measurement unit for changes of the electronic parameters of the components with fluctuations of the operating conditions (e.g. forward current through the LED and temperature) a reference light source is used (HLMA-KL00-I0000 (Avago Technologies US Inc.). The excitation light of the LED was sine wave modulated at a frequency *f* of 20 kHz.

3.2 Optical fiber tip micro fabrication by chemical etching

The most efficient configuration of optical fibre for collecting the luminescence emission and to reduce the optical background was achieved by coating the sensitive layers onto the sharpened tip of optic cables with core diameter of 400 and 200 µm. For this purpose the fiber tips have been micro-machined by chemically etching process (tube etching) of multi-mode optical fibers (Si core and hard polymer cladding, Thorlabs). The schematic illustration of the forming of a sharpened fiber tip is presented in Fig. 9. After the etching process was completed, the tip of the optical fiber was rinsed with distilled water and cleaned with acetone. The height of the obtained cone tip is about 1.5 mm. All the etching experiments were carried out at room temperature. The obtained form of an optical fibre efficiently resulted in improved signal-to-noise ratio of about one order of magnitude for both types of sensors thus resulted in an increased luminescence signal.

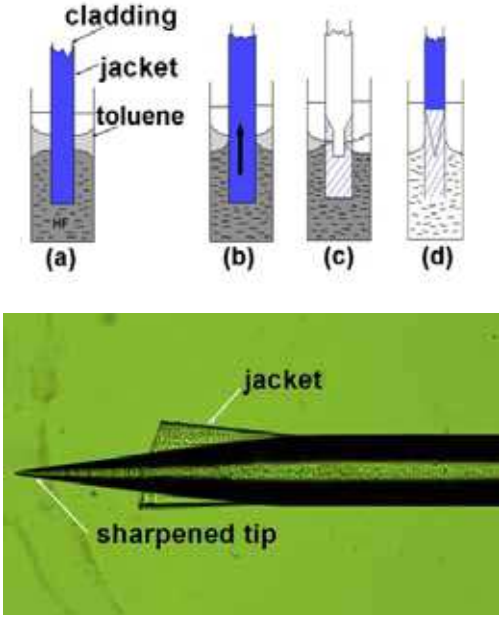

Fig. 9. Top: (a) immersion of a fiber tip into the etchant-organic solution (40 % hydrofluoric acid-toluene); (b) pull out of the fibre until a meniscus is formed at the interface; (c) the meniscus height reduces progressively until the portion of the fiber below the organic solvent is completely etched (d). Below: formed a cone-shaped tip with an angle between 15 – 20 °.

3.3 Preparation of O_2 fiber optical sensor

The sensitive cocktail is composed of Pt-TFPP dissolved in polystyrene (4 w. % dye/g solid polystyrene in chloroform). The optical fibres were coated by dipping only the sharpened tip of the fibre into a sensitive cocktail. After coating, the oxygen sensors have been dried at 60 °C for eight hours.

3.4 Preparation of CO_2 sensing cocktail

The carbon dioxide sensitive cocktails were prepared by mixing donor and acceptor dye, along with a phase transfer agent, tetraocytlammonium hydroxide (TOAOH) in ethylcellulose solution and coating a sensitive thin film onto the tip of etched optical fiber. The polymer solution of ethyl cellulose (EC) was prepared by dissolving 4.4 g of EC in the 40 g of a toluene/ethanol mixture (80/20, v/v), giving a viscous 11 % (w/w) solution. Ru(dpp) nanobeads incorporated in oxygen impermeable polymer, polyacrilonitrile (PAN) have been suspended in polymer (EC) solution. Acceptor was prepared by dissolving 2.03 mg of phenol red (PR) in 1.5 ml of toluene/ethanol mixture to which 20 µl of TOA-OH (20 % solution in methanol) solution was added. The rate of energy transfer and therefore the sensitivity of the sensor are almost independent of the concentration of the donor in the matrix. However, an increase in donor concentration enhances the luminescence intensity and therefore the signal-to-noise ratio. In contrary, the concentration of the deprotonated form of acceptor is a decisive factor upon which the rate of energy transfer strongly depends since the overlap integral is proportional to the concentration of the acceptor in Förster equation. Owing to this, the signal change depends not only on the degree of protonation by carbon dioxide but also on the overall concentration of the acceptor in the sensor membrane. Therefore, the final cocktail composition consisted of 13.8 mmol Ru(dpp) and 3.08 mmol PR per kg of solid polymer. The cocktails were saturated with carbon dioxide before coating of the fiber tip. The resulting fiber optical sensors were dried for 4 hours at 70 °C before an additional ion impermeable layer of Teflon with added black graphite as an optical and protective isolation was applied. The dried sensors were stored in desiccator over sodium carbonate before use. Before the calibration was proceeded the optical fibers have been exposed to solution equilibrated with CO_2 (20 %) and N_2 in order to obtain faster stable response of the sensor.

3.5 Measuring principle of CO_2 optical sensor

For the realisation of an optical lifetime-based CO_2 sensor, whose luminescence and lifetime are modulated by pH dependent efficiency of resonance energy transfer, some criteria need to be considered at selection suitable donor-acceptor pairs: (a) a pH-sensitive indicator is combined with long-lived transition metal complex; (b) an absorbance spectrum of deprotonated form of analyte dependent pH-indicator has to overlap with the luminescence spectrum of the inert luminophore, added as a donor so that efficient energy transfer takes a place; (c) the distance between donor and acceptor does not exceed Förster distance (in the range 1-10 nm), (d) lifetime of the donor in microsecond range (e) high quantum yield of the donor and (f) excitation of the acceptor and donor at a single band of wavelength and detection of donor luminescence at a common wavelength using a single photodetector. In order to convert a change in absorption spectrum of acceptor in presence of CO_2 into lifetime

information, a long-lifetime luminescent donor need to be co-immobilised in the same matrix. Depending on the pH, the acceptor changes its colour and deactivates the excited state of the donor. This effect changes both the luminescence intensity and the lifetime of the donor. Ru(II) diphenyl-phenanthroline (Ru(dpp)) was selected as a donor due to the high quantum yield (0.6) and long lifetime in range of microseconds (~ 5.5 µs). Its absorption spectrum perfectly overlaps the emission of bright blue LEDs and its red emission spectrum overlaps the absorption of the deprotonated form of pH-indicators in red region of spectrum. Among the investigated pH indicators the main problem was their poor photostability (for example for the case of cresol purple and bromothymol blue) and due to the pronounced photobleaching these indicators turned out to be not suitable for the fiber optic measurement system. Even the strategy of optimising the ratio between the concentrations of pH indicator in comparison to the concentration of the donor did not allow realising a sensor with satisfactorily stability properties. Therefore on the basis of enough overlapping of the absorption spectrum of deprotonated form of phenol red (i.e. in absence of CO_2) with luminescence of Ru(dpp) phenol red was chosen as an acceptor (Fig. 10) . This dye provides enough intensity when the energy transfer with Ru(dpp) takes place, has pK_a value in the physiological range (6.8) and expand the measurement range up to 20 % of CO_2 (corresponding to 147 mmHg).

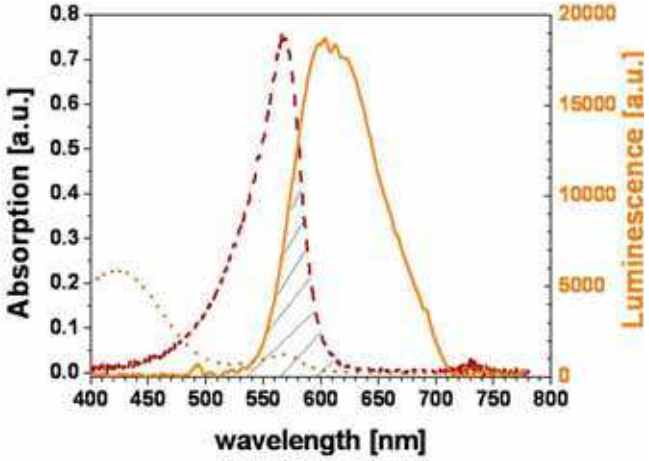

Fig. 10. Luminescence emission spectrum of $Ru(dpp)_3^{2+}$ (solid line) and absorption spectra of phenol red in the absence (dashed line) and presence (dotted line) of CO_2 (20 %). The hatched area indicates the spectral overlap of the donor emission and acceptor absorption.

The CO_2 sensor is solid type sensor, what means that no buffer was used. Instead this the pH indicator (A) forms a hydrated ion-pair ($A^-Q^+ xH_2O$) by an addition of quaternary ammonium base (Q^+OH^-) (Mills et al., 1992). To stabilize the deprotonated form of the indicator dye in the matrix and to form a lipophilic bicarbonate buffer system in the polymer, tetraoctyl ammonium hydroxide was used. The excess amount of TOA-OH is neutralised by atmospheric carbon dioxide to form a lipophilic hydrogen carbonate buffer in the solid matrix, and this can tune the sensitivity and improve the storage stability of the sensor. The sensing mechanism of an acceptor-Q^+OH ion-pair is described by (3):

$$TOA^+A^-.xH_2O + CO_2 \leftrightarrow TOA^+HCO_3^-.(x-1)H_2O + AH \quad (3)$$

where $[TOA^+A^-.xH_2O]$ is the complex of the deprotonated pH indicator dye ion paired with the quaternery ammonium cation TOA^+ and a number x means the hydrophilic sites present in the polymer matrix.

In the case of Resonance Energy Transfer (RET) as sensing scheme the average lifetime is converted into a parameter (phase angle) that reflects the concentration of deprotonated pH-indicator (acceptor). The CO_2 dependent lifetime information is detected using the technique of phase fluorometry. In this technique, the lifetime data (τ) are converted to phase shift data (ϕ) as it was described by equation (1).

Efficiency of energy transfer E is expressed as:

$$E = \frac{k_{RET}}{k_{RET} + k_{other}} = 1 - \frac{\tau_{max}}{\tau} \quad (4)$$

where k_{RET} is rate of resonance energy transfer and k_{other} is the sum of the rates of all other deactivation processes including luminescence. τ_{max} reflects the lifetime of donor (complete protonation of acceptor at very high pCO_2, when no energy transfer occurs) and τ is a lifetime in the absence of carbon dioxide. By rearrangement of the equation 4 the ratio τ_{max}/τ can be expressed as:

$$\frac{\tau_{max}}{\tau} = \frac{k_{other} + k_{RET}}{k_{RET}} = 1 + \frac{k_T}{k_F} \quad (5)$$

From Förster theory it follows, that the rate of energy transfer k_T is proportional to the spectral overlap integral J between donor emission and acceptor absorption ($k_T \propto J$). When the pH-indicator is completely completely protonated, there is no spectral overlap with the donor and overlap integral J is proportional to concentration of deprotonated dye D^-:

$$\frac{\tau_{max}}{\tau} - 1 = \frac{k_{RET}}{k_{other}} \cong J \cong \left[D^-\right] \quad (6)$$

This model corresponds to the situation of dynamic quenching of luminescence described by the Stern-Volmer equation. Therefore pCO_2 was calculated from the measured phase shift of the luminescence using as described by equation (7):

$$\phi = \phi_0 \left[\frac{f_0}{1 + K \cdot pCO_2} + 1 - f_0\right] \quad \phi = \phi_0 \left[\frac{f_0}{1 + K \cdot pCO_2} + 1 - f_0\right] \quad (7)$$

3.6 Laboratory calibration protocol

Before of the *in vivo* measurements, the fiber optical pO_2 and pCO_2 sensors have been calibrated in laboratory. In the case of pO_2 sensors, a glass vessel filled with Ringer solution and kept in a water bath (Lauda RC 6 CP thermostat) at the constant temperature of 37 °C has been equilibrated with a gas mixture of nitrogen/oxygen at defined

concentrations (typically 0, 5, 10 and 21 % O_2) using a mass flow controller (Bronkhorst, The Netherlands). Similarly, in the case of the pCO_2 sensors the Ringer solution has been equilibrated with a gas mixture of nitrogen/carbon dioxide at defined concentrations (typically 0, 5, 10, 15 and 20 % CO_2). A gas purity analyzer (Servomex) with both a paramagnetic O_2 sensor and a CO_2 infrared sensor has been used as reference to analyse the composition of the gas mixture dissolved in the Ringer solution. The fiber optic sensors have been put in contact with the Ringer solution and the phase shift at each defined gas concentration has been recorded. An example of the phase shift response at exposed gas concentration is shown in Fig. 11 for pO_2 sensors and in Fig. 12 for pCO_2 sensors, respectively. It can be seen that for both sensors usually two cycles of dissolved O_2 and CO_2 concentrations have been measured. The first cycle has been used for sensor calibration purpose, whereas the following cycle is used to check the specifications of the oxygen and carbon dioxide measurements calculated with calibration parameters obtained from equations 2 and 7, respectively.

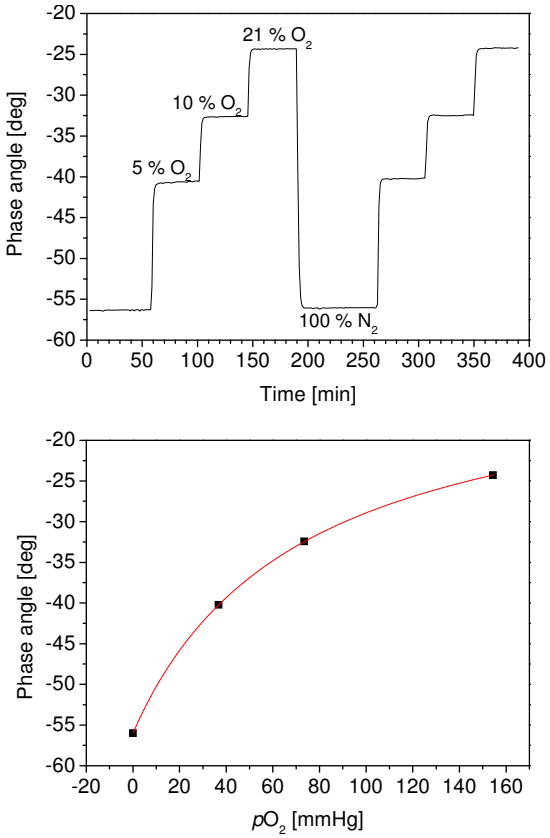

Fig. 11. Oxygen sensor response curve, phase angle as a function of different O_2 concentrations; below: calibration curve obtained by the first cycle of dissolved oxygen concentrations.

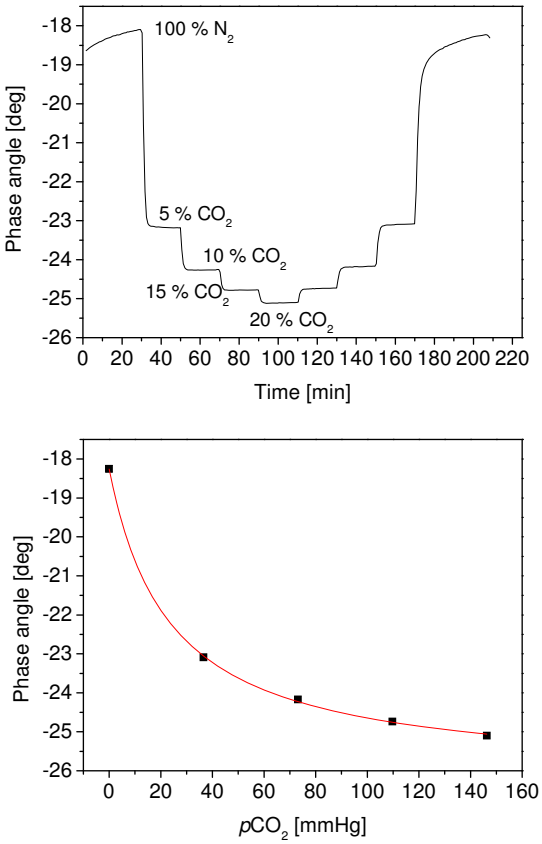

Fig. 12. Carbon dioxide response curve, phase angle as a function of different CO_2 concentrations; below: calibration curve obtained by the first cycle of dissolved CO_2 concentrations.

3.7 *In vivo* pO_2 and pCO_2 measurements on animal by use of fiber optical sensors

In vivo experiments on test animals have been performed at the Medical Univeristy Graz, Clinical Department of Heart Surgery. Fourteen pigs (30.7 $\pm$ 2.5 kg) were investigated by monitoring the pO_2 and pCO_2 content in tissue of the three vital organs: brain, heart and liver in order to examine the oxygen delivery to the tissue of these organs during simulated heart surgery operations. Heart surgery intervention is necessary to heal and treat cardiac defect or valvular heart diseases. During this kind of surgeries an extracorporeal blood circulation can be carried out using the so-called "heart lung machine" (HLM) which temporarily takes over the functions of the heart and lungs during surgeries, maintaining the circulation of blood in the body. A heart lung machine maintains perfusion to other body organs and tissues while the surgeon works in a bloodless surgical field.

The aim of test on animals was the simultaneously evaluation of pO_2/pCO_2 exchanges in three vital organs: brain, heart and liver using two different methods of extra corporal

circulation: conventionally cardiopulmonary bypass (CPB) and Minimal Extra Corporal Circulation (MECC) (see Fig. 13). The questions that appeared were: are the optical fiber sensors suitable for the evaluation of metabolic variables and organ specific O_2/CO_2 exchanges during heart surgery and furthermore, is it on the basis of the obtained results capable to estimate difference between CPB and MECC?

Fig. 13. CPB (left) and MECC (right)

3.7.1 Experimental protocol

pO_2 and pCO_2 have been measured continuously with fiber optical sensors previously calibrated in laboratory and checked again before the *in vivo* measurements, directly at the place of the in vivo measurements. In order to protect the fragile tip of the optical fibers and to position the two type of sensors as near as possible to each other at the local place of the measurement, each sensor (one pO_2 and one pCO_2) was inserted in the needle (inner diameter of 500 mm) and then implanted into the tissue of the organ. Firstly, a drill hole has been made in temporal region of the skull above ear in order to insert a needle containing the optical pO_2 and pCO_2 sensors deeply into the brain tissue. In this region is the skull of pigs thinnest due to the thickness of bones. Afterwards was the thorax and abdomen opened to insert the optical sensors into the liver and finally into heart tissue. After baseline measurements (recording of the first blood values and the first values obtained with the optical sensors) the aorta was cross clamped for a period of 60 min and the HLM was put into operation. The blood values and the tissue values of pO_2 and pCO_2 have been taken at intervals of time of 15 minutes. After one hour of operation the clamps of the HLM have been removed and the heart has been reanimated for 30 minutes. The physical state of the animal has been monitored another half of hour before the experiment ended. The exact study protocol is shown in Table 2:

Time	Event
T_1	Baseline before connection of HLM under physiologic conditions
T_2	During cooling on HLM after 15 min (then cross clamping of aorta)
T_3	15 min after cross clamping the aorta
T_4	30 min after cross clamping the aorta
T_5	45 min after cross clamping the aorta (then rewarming)
T_6	60 min after cross clamping the aorta (then de clamping of aorta)
T_7	15 min after normothermic reperfusion
T_8	30 min after normothermic reperfusion (off-HLM)
T_9	15 min after end of using of HLM
T_{10}	30 min after end of HLM (end of experiment)

Table 2. Protocol of *in vivo* experiments

3.7.2 Results of *in vivo* experiments

Since the brain tissue perfusion is one of the most important substrate for energy metabolism delivered by the blood, an example of pO_2 and pCO_2 profiles measured by fiber optical sensor in this organ are shown in Fig. 14. Despite the very low pO2 values at the beginning of the measurement, a slightly decrease in pO_2 value during HLM can be observed, followed by an increase up to 55 mmHg during recirculation. On the contrary, pCO_2 increases up to 40 mmHg during HLM and after recirculation reaches the same value as at the beginning (10 mmHg). These measurements confirmed a heterogeneous distribution of local pO_2 and pCO_2 values in brain. The tissue concentration is determined by the balance between supply and utilisation and the anatomical distribution of concentration and within the brain was reported to be wide, depending on the depth of penetration of the sensor into the tissue (Luebbers & Baumgaertl, 1997). The pO_2 and pCO_2 responses as shown in Fig. 14 have an opposite trend which is in agreement with medical point of view that anaerobic condition of tissue correlate with increase of CO_2 content.

The supply of brain with oxygen depends on the cerebral perfusion and on difference between arterial and venous O_2 partial pressures. CO_2 partial pressure has a significant influence on the blood circulation in the brain. When the arterial CO_2 partial pressure p_aCO_2 increases, pCO_2 in brain increases proportional with this increment. If on the contrary Hyperventilation causes a decrease of pCO_2 down to 20 mmHg, than a cerebral Hypoxia and increased cerebral Lactacidose is provoked due to the vasoconstriction.

Despite the fact that brain are very active organ with higher oxygen and energy demand, low pO_2 values below 10 mmHg has been often measured. Such sensor behavior could be obtained due to the influence of the narcosis on the brain activity and due to the position of the sensor tip in brain. Latter can result in holes by implantation of the optical sensor probes into brain region since the brain consists of the tissue and the hollow spaces. As a consequence of the positioning of the optical fiber in hollow spaces, lower pO_2 values can be obtained during measurements in brain.

Fig. 15 and 16 show oxygen and carbon dioxide profile in liver and heart, respectively. In vivo measurements in liver reflected lower pO_2 values before HLM was put into an operation (pO_2 values app. 5 mmHg) and afterwards a decrease of pO_2 vales in the range of 1.5 mmHg. After corporal recovery, the pO_2 values reach the value at the beginning of the

measurement. Similarly, pCO_2 values in liver are at beginning of 8 – 10 mmHg, and during HLM operation an increase in pCO_2 has been noticed (app. 13 mmHg). After recirculation pCO_2 reaches the values similar at the beginning of the experiment (8 mm Hg).

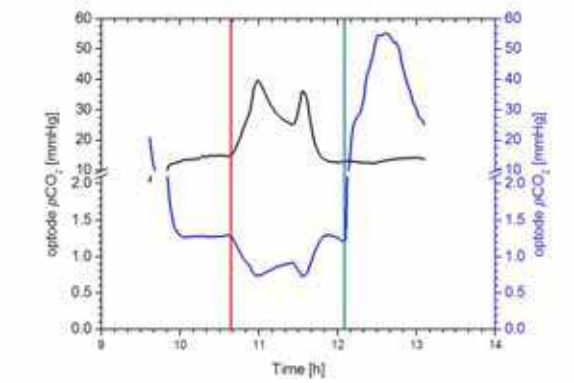

Fig. 14. *In vivo* measurement in brain obtained with inserted pO_2 and pCO_2 fiber optical micro sensors: red line indicates the start of functionality of HLM, while green line indicates the return to the normal intra-corporeal circulation. The x scale shows the real time of the measurement, so it can be seen that the experiment has started at about 9:30 am and ended few minutes after 13:00 for an overall duration of less than 4 hours.

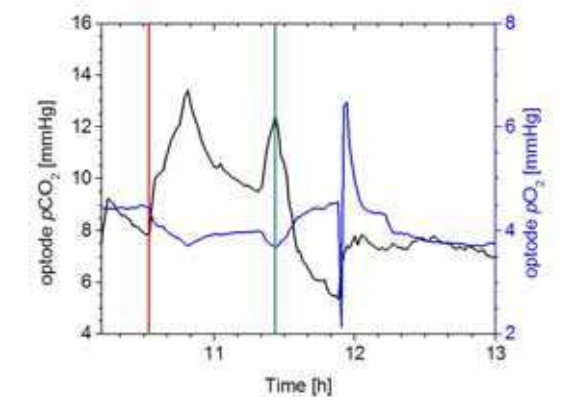

Fig. 15. *In vivo* measurement in liver obtained with inserted pO_2 and pCO_2 fiber optical micro sensors: red line indicates the start of functionality of HLM, while green line indicates the return to the normal intra-corporeal circulation.

For the comparison of all performed *in vivo* experiments on animals using either CPB or MECC as extracorporeal circulation system the measured pO_2 and pCO_2 values were statistically arranged with a two way analysis of variance (ANOVA) model. The measured parameters were normalized to the initial values at a level of 100 % due to the high variances of initial values of those variables measured with optical sensors (pO_2, pCO_2). Those results are shown in Fig. 17 to 19 for the brain, liver and heart, respectively.

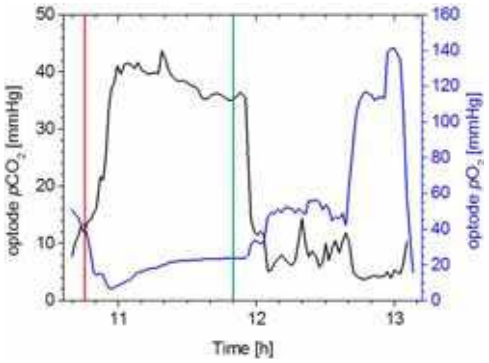

Fig. 16. *In vivo* measurement in heart obtained with inserted pO_2 and pCO_2 fiber optical micro sensors: red line indicates the start of functionality of HLM, while green line indicates the return to the normal intra-corporeal circulation.

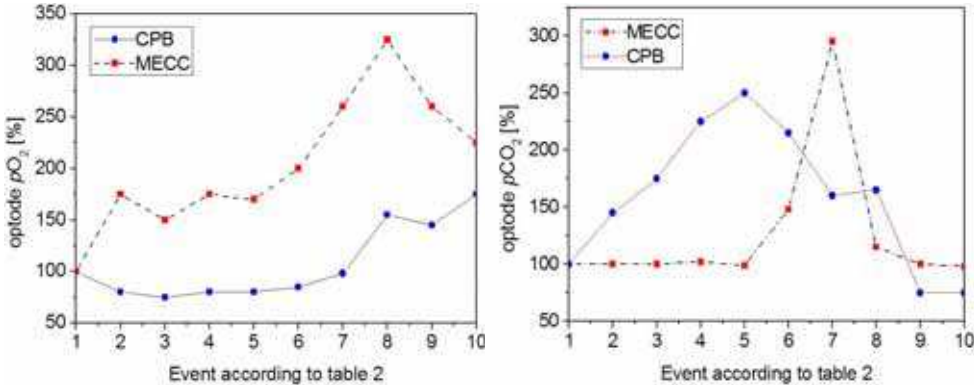

Fig. 17. Comparison of the values measured with optical fibers and normalized to the initial values at a level of 100 % for *in vivo* measurements in brain.

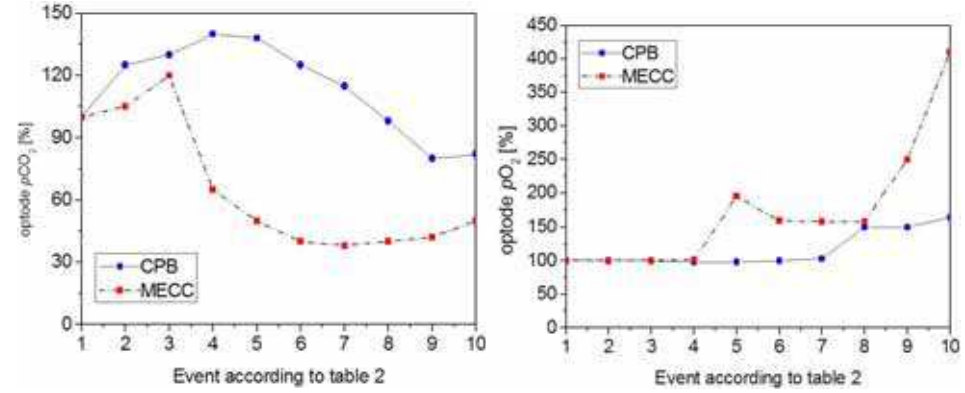

Fig. 18. Comparison of the values measured with optical fibers and normalized to the initial values at a level of 100 % for *in vivo* measurements in liver.

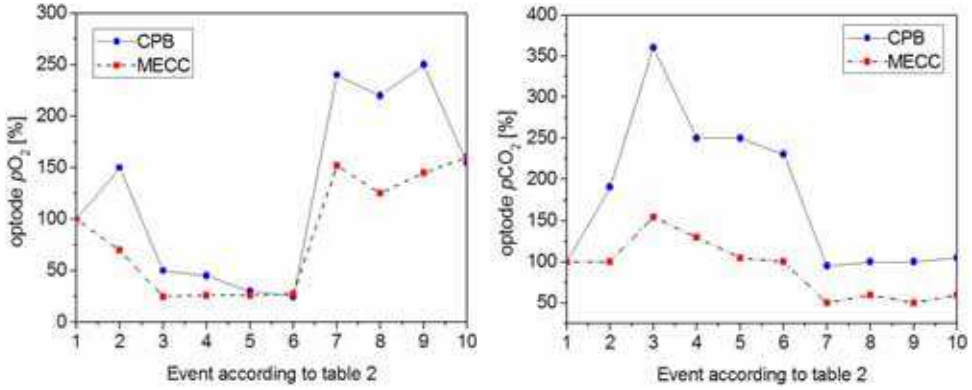

Fig. 19. Comparison of the values measured with optical fibers and normalized to the initial values at a level of 100 % for *in vivo* measurements in heart.

The above Figures indicate on the similar trends of pO_2 and pCO_2 curves for both extracorporeal circulation systems. It is shown that under standardised conditions pO_2 curves in brain were absolutely higher in the case of mini-ECC. In the case of liver it was found that under standardised conditions intrahepatic parenchymal pCO_2 curves were absolutely higher and they are significantly correlated to arterial and central venous lactate in CPB.

3.8 Conclusions

In the presented work a novel combined optochemical measurement system which allows a simultaneously measurement of dissolved oxygen and carbon dioxide in tissue of vital organs is described. The tissue oxygenation is frequently monitored with electrochemical micro sensors (e.g. polarographic needle electrodes) which one limitation is that due to the oxygen consumption during pO_2 measurements, the probe needs to be moved through the tissue (Lowry & Fillenz, 2001; Luebbers, 1996, Nair, 1987). On the contrary fiber optic probe can be left in the same position in the tissue for a prolonged period of time because is non-invasive. This makes it possible to directly temporal changes in pO_2 as well as the oxygenation-modifying interventions over time in a tissue. Furthermore, optochemical sensors based on luminescence intensity show higher sensitivity and the use of phase modulation fluorometry as measuring techniques for both oxygen and carbon dioxide sensors enable the realisation of optical sensors with excellent characteristics of reliability and measurement stability possible superior to those of electrodes. Further advantage of optical sensors over the electrodes is ease of miniaturisation. In presented work tapered optical fiber tips obtained through chemically etching improved the signal-to-noise ratio of about one order of magnitude. Based on this fact further miniaturisation can be achieved, using a fiber optical cables with smaller diameter (e.g. 50 μm). This type of the optical sensors also offers a possibility to use them for endoscopy. Furthermore, the described optical sensors are almost calibration free using only one point recalibration.

Despite the fact, that the last years are witnessed to an increased number of optochemical oxygen sensors based on phase modulation fluorometry in field of medical applications, especially for analysing the spatial heterogeneity in oxygen tension in tumor tissue using optical oxygen probes OxyLite (Oxford Optronix, Oxford, UK), at present and up to our

knowledge there has been no reports about fiber optical CO_2 sensors for measuring pCO_2 content in tissue of organs.

The described optochemical instrumentation has been used in in vivo tests for simultaneously detection of oxygen and carbon dioxide exchange in brain, heart and liver using two different methods as extra corporal circulation: Minimal Extra corporal Circulation (MECC) and Cardiopulmonary bypass (CPB). It has been turned out that a significantly higher demand of blood transfusion is required and higher lactate values (correlated to higher pCO_2 values) are observed when using classical method CPB. The continuous acquisition of metabolic parameters (pO_2 and pCO_2) has showed that in the case of using MECC as extra corporal circulation, significantly higher pO_2 values are obtained, while the use CPB resulted in significantly higher pCO_2 in liver and heart tissue.

It is demonstrated that with a help of miniaturised non-invasive fiber optical sensors for continuously measurement of tissue pO_2 and pCO_2 a significant better O_2/CO_2 metabolism is achieved in the case of MECC as extra corporal circulation. Furthermore, MECC produced less lactate and showed significantly favourable results concerning O_2/CO_2 metabolism and transfusion demand.

4. Acknowledgement

The research work was part of the Zukunftsfonds funded by the Styria Country Government A3 Science and Research, Reference A3-22M1/206-4. The aim of this project was to develop a combine optochemical measurement system for determination of oxygen and carbon dioxide for medical applications.

The tests on animals have been made in cooperation with Univ. Prof. Dr. Igor Knez and Dr. med. univ. Elisabeth Beran at the Medical Univeristy of Graz, Clinical Department for Heart Surgery (Austria).

5. References

Astrup, P. & J. Severinghaus, W. (1986). *The Hystory of blood gases, Acids and Bases*, Munksgaard, Copenhagen, 1st ed.

Bizzarri, A.; Koehler, H.; Cajlakovic, M.; Pasic, A.; Schaupp, L.; Klimant, I. & Ribitsch, V. (2006). Continuous oxygen monitoring in subcutaneous adipose tissue using microdialysis. *Analytica Chimica Acta*, Vol. 573-574, (July 2006) pp. 48-56.

Bizzarri, A.; Konrad, C.; Čajlaković, M. & Ribitsch, V. (2007). New developments of an optochemical measurement system for the continuous monitoring in subcutaneous tissue by microdialysis. *Proceedings IEEE Sensors 2007*, (October 2007), Atlanta, USA.

Cajlakovic, M.; Bizzarri, A. & Ribitsch, V. (2006). Luminescence lifetime-based carbon dioxide optical sensor for optical applications. *Analitica Chimica Acta*, Vol. 573-574, (July 2006) pp. 57-64.

Cajlakovic, M.; Bizzarri, A.; Suppan, M.; Konrad, C. & Ribitsch, V. Continuous monitoring of pO_2 and pCO_2 by microdialysis indicates physiologic status of the critically ill patients. (2009). *Sensors and Actuators B*, Vol. 139, Issue 1 (May 2009) pp. 181-186.

Chang, P. P.; Sussman, M. S.; Conte, J. V.; Grega, M. A.; Schulman, S. P.; Gerstenblith, G.; Wang, N. Y.; Capriotti, A.; Weiss, J. L. (2002) Post-operative ventricular function, and cardiac enzymes after on-pump versus off-pump CABG surgery. *American Journal Cardiology*, Vol. 89 (2002) pp.1107—1110.

Cooney, C. G. & Towe, B. C. (1997). Intravascular carbon dioxide monitoring using micro-flow colorimetry. *Biosensors and Bioelectron*ics, Vol. 12, No.1, (January 1997) pp. 11.

Cooney C. G.; Towe, B. C. & Eyster, C. R. (2000). Optical pH, oxygen and carbon dioxide monitoring using a microdialysis approach. *Sensors & Actuators* , Vol. 69 (September 2000), pp. 183.

Goossens, G. H.; Bizzarri, A.; Venteclef, N.; Essers, Y.; Cleutjens, J. P.; Konings, E.; Jocken, J. W. E.; Cajlakovic, M.; Ribitsch, V.; Clément, K & Blaak E. E. (2011). Adipose tissue hyperoxia is accompanied by insulin resistance, impaired adipose tissue capillarisation and inflammation in obese men. *Circulation*, (July 2011) pp. 1-10.

Goossens, G. H; Saris W. H. M. & Blaak E.E. Microdialysis on Adipose Tissue. In: Tsai, T-H, ed. Applications of Microdialysis in Pharmaceutical Science. Hoboken, NJ: John Wiley & Sons, Inc., *In press*..

Hahn, C. E. W. (1998). Electrochemical Analysis of Clinical Blood-gases, Gases and Vapours. *Analyst*, Vol. 123, (June 1998), pp. 57R-86R.

Harsten, A.; Berg, B.; Inerot, S. & Muth, L (1988). Importance of correct handling of samples for the results of blood gas analysis. *Acta Anaesthesiologica Scand*inavica, Vol. 32 (1988), pp. 365-368.

Hou, H.; Grinberg, O. Y.; Taie, S.; Leichtweis, S.; Miyake, M.; Grinberg, S.; Xie, H.; Csete, M. & Swartz, H. M. (2003). Electron Paramagnetic Resonance Assessment of Brain Tissue Oxygen Tension in Anesthetized Rats. *Anesthesia & Analgesia*, Vol. 96, (May 2003), pp. 1467–1472.

Immer, F. F.; Pirovino, C.; Gygax, E.; Englberger, L.; Tevaearai, H.; Carrel, T. P. (2005). *Minimal versus Conventional cardiopulmonary bypass: assessment of intraoperative myocardial damage in coronary bypass surgery*, Vol. 28, Nu. 5 (November 2005) pp. 701-704.

Kamiya, H.; Kofidis, T.; Haverich, A. & Klima. (2006). Preliminary experience with the mini-extracorporeal circulation system (Medtronic resting heart system). Interactive Cardio Vascular and Thoracic Surgery, Vol. 5, No. 6 (August 2006) pp. 680-682.

Kofidis, T.; Baraki, H.; Singh, H.; Kamiya, H.; Winterhalter, M. & Didilis. (2008). The minimized extracorporeal circulation system causes less inflammation and organ damage. *Perfusion*, Vol. 23, No. 3 (May 2008) pp. 147-151.

Lakowicz, J.R. (1983). Principles of Fluorescence Spectroscopy, Plenum Press, New York, London, 1983, pp. 257.

Levy, J.H.; Tanaka, K. A. (2003) Inflammatory response to cardiopulmonary bypass. *Annual Thoracic Surgery*, Vol. 75 (2003) pp. 715—720.

Lowry, J. P. & Fillenz, M. (2001). Real-time monitoring of brain energy metabolism in vivo using microelectrochemical sensors: the effects of anesthesia. *Bioelectrochemistry*, Vol. 54, (August 2001) pp. 39-47.

Luebbers, D. W. (1996). Oxygen electrodes and optodes and their application in vivo. *Advances in Experimental Medicine and Biology*, Vol. 388, (October 1996) pp.13-34.

Luebbers, D. W. & Baumgaertl, H. (1997). Heterogenities and profiles of oxygen pressure in brain and as Examples of the pO_2 distribution in the living tissue. *Kidney International*, Vol. 51, (February 1997) pp. 372-380.

Maldonado, F. A; Weil, M. H.; Tang, W.; Bisera, J.; Gazmuri, R.; Johnson, B. & D´Alessio A. (1993). Myocardial Hypercarbic Acidosis educes Cardiac Resuscitability. *Anesthesiology*, Vol. 78, No.2, (February 1993), pp. 343-352.

Mills, Q.; Chang, A. & McMurray, N. (1992). Equilibrium study on colorimetric plastic film sensors for carbon dioxide. *Analytical Chemistry*, Vol. 64, No. 13 (July 1992) pp. 1383-1389.

Nair, P. K.; Buerk, D. G. & Halsey, J. H. (1987). Comparison of oxygen metabolism and tissue pO_2 in cortex and hippocampus. *Stroke*, Vol. 18, No. 3 (May-June 1987) pp. 616-622.

Pasic, A.; Koehler, H., Schaupp, L.; Pieber, T. R. & Klimant, I. Fiber-optic flow-through sensor for online monitoring of glucose. (2006). *Analytical and Bioanalytical Chemi*stry, Vol. 386, No. 5, (October 2006) pp. 1293.

Pentila,¨ H. J; Lepoja¨rvi, M. V. K.; Kiviluoma, K. T.; Kaukoranta, P. K.; Hassinen, E.; Peuhkurinen, K.J. (2001) Myocardial preservation during coronary surgery with and without cardiopulmonary bypass. *Annual Thoracic Surgery*, Vol. 71 (June 2001) pp. 565—71.

Rosser, D. M.; Stidwill, R. P.; Jacobson, D. & Singer, M. (1995). Oxygen Tension in the Bladder Epithelium Rises in Both High and Low Cardiac Output Endotoxemic sepsis. *Journal of Applied Physiology*, Vol. 79 (December 1995), pp. 1878-1882.

Rosser, D. M.; Stidwill, R. P.; Jacobson, D. & Singer M. (1996). Cardiorespiratory and Tissue Oxygen Dose Response to Rat Endotoxemia. *Heart and Circulatory Physiology*, Vol. 271, (September 1996), pp. H891- H895.

Suzuki, H.; Arakawa, H.; Sasaki, S. & Karube, I. (1999). Micromachined Severinghaus-type carbon dioxide electrode. *Analytical Chemistry*, Vol.71 (May 1999), pp. 1737-1743.

Suzuki, H., Hirakawa, T.; Hoshi, T. & Toyooka, H. (2001). Micromachined sensding module for pO_2, pCO_2 and pH and its design optimization for practical use. *Sensors and Actuators B*, Vol. 76 (June 2001), pp. 565-572.

Tang, W.; Weil, M.; Gazmuri, R.; Bisera, J. & Rackow (1991). Reversible Impairment of Myocardial Contractility due To Hypercarbic Acidosis in the Isolated Perused Rat Heart. *Critical Care Medicine*, Vol. 19, No.2, pp. 218.

Tsukada, K.; Sakai, S.; Hase, K. & Minamitani, H. 82003). Development of catheter-type optical oxygen sensor and applications to bioinstrumentation. *Biosensors and Bioelectronics*, Vol. 18 (October 2003), pp. 1439-1445.

Tusa, J. K. & Leiner, M. J. (2001) Fluorescent optical sensor for critical care analytes. *Annals de Biologie Clinique*, Vol. 61, (September 2001), pp. 183-191.

Ungerstedt, U. (1991). Microdialysis-principles and applications for studies in animals and man. *Journal of Internal Medicine*, Vol. 230, No. 4, (October 1991) pp. 365.

Vollmar, B.; Conzen, P. F.; Kerner, T.; Habazettl, H.; Vierl, M.; Waldner, H. & Peter, K. (1992). Blood Flow and Tissue Oxygen Pressures of Liver and Pancreas in Rats: Effects of Volatile Anesthetics and of Hemorrhage. *Anesthesia & Analgesia*, Vol. 75, (September 1992), pp. 421-430.

Whitehouse, T.; Stotz, M.; Taylor, V.; Stidwill, R.& Singer, M. (2006). Tissue Oxygen and Hemodynamics in Renal Medulla, Cortex and Corticomedullary Junction During Hemorrhage-Reperfusion. *American Journal of Physiology – Renal Physiology*, Vol. 291, (March 2006), pp. F647-F653.

Wolfbeis, O. S.; (1991). From fluorescent probes to optical sensors, *Analytical Proceeding*, Vol. 28 (1991), pp. 357.

Ye J.; Gao Z.; Yin J.; He Q.(2007). Hypoxia is a potential risk factor for chronic inflammation and adiponectin reduction in adipose tissue of dietary obese mice. *American Journal of Physiology*, Vol. 293, No. 4, E1118-1128.

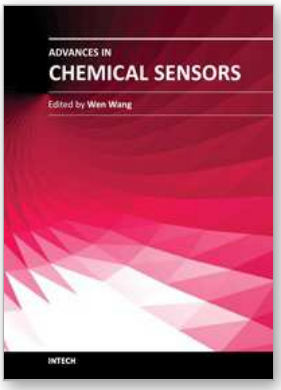

Advances in Chemical Sensors

Edited by Prof. Wen Wang

ISBN 978-953-307-792-5
Hard cover, 358 pages
Publisher InTech
Published online 20, January, 2012
Published in print edition January, 2012

The chemical sensor plays an essential role in the fields of environmental conservation and monitoring, disaster and disease prevention, and industrial analysis. A typical chemical sensor is a device that transforms chemical information in a selective and reversible way, ranging from the concentration of a specific sample component to total composition analysis, into an analytically useful signal. Much research work has been performed to achieve a chemical sensor with such excellent qualities as quick response, low cost, small size, superior sensitivity, good reversibility and selectivity, and excellent detection limit. This book introduces the latest advances on chemical sensors. It consists of 15 chapters composed by the researchers active in the field of chemical sensors, and is divided into 5 sections according to the classification following the principles of signal transducer. This collection of up-to-date information and the latest research progress on chemical sensor will provide valuable references and learning materials for all those working in the field of chemical sensors.

InTech Europe
University Campus STeP Ri
Slavka Krautzeka 83/A
51000 Rijeka, Croatia
Phone: +385 (51) 770 447
Fax: +385 (51) 686 166
www.intechopen.com

InTech China
Unit 405, Office Block, Hotel Equatorial Shanghai
No.65, Yan An Road (West), Shanghai, 200040, China
中国上海市延安西路65号上海国际贵都大饭店办公楼405单元
Phone: +86-21-62489820
Fax: +86-21-62489821